*Int. J. Electrochem. Sci.*, 7 **(2012)** 4898 - 4917

International Journal of
ELECTROCHEMICAL
SCIENCE
www.electrochemsci.org

# Electrochemical and Mechanical Properties of Mild Steel Electro-plated with Zn-Al.

*A.P.I Popoola*[*]*, O.S.I Fayomi and O.M Popoola.*

Faculty of Engineering and the Built Environment, Tshwane University of Technology, Private Bag X680, Pretoria 0001, South Africa.
[*]E-mail: popoolaapi@tut.ac.za; sunnyfayomi@yahoo.com

*Received:* 17 April 2012 / *Accepted:* 1 May 2012 / *Published:* 1 June 2012

Surface enhancement of engineering materials is necessary for preventing service failure and corrosion attack in the industries. Deposition was performed to obtain a better surface adherent coating using electroplating technique. Zn-Al film was developed with zinc and aluminum powder particles dissolved in nitric acid and sodium hydroxide respectively, to form solutions containing $Zn^{2+}$ and $Al^{3+}$ ions. Anomalous co-deposition on mild steel resulted into surface modification attributed to the complex alloys that was developed. The effect of deposition potential was systematically studied using Focused-ion beam scanning electron microscope (FIB-SEM), Atomic force microscope (AFM), X-ray diffraction (XRD) and Fourier transform infra-red (FTIR). Thick, adherent, smooth and uniform Zn-Al coating was deposited with relatively high deposition rate of 1.0 V. Experimental results indicated that the introduction of Al into the coating does significantly alter the chemical and mechanical properties of the mild steel. The microhardness value was increased by 92%; wear rate was decreased by 90% and a significant increase in the corrosion resistance was achieved based on the formation of stable deposited particles of Zn-Al.

**Keywords:** Surface enhancement, composite, co-deposition, corrosion study.

## 1. INTRODUCTION

Electroplating of Zinc on mild steel plate is widely used to provide corrosion protection (1-6). However, since the protection offered by Zn coatings cannot be guaranteed under severe chloride and acidified conditions (5-9), alternative method and materials have been carefully studied. Among this materials are the Zn–Ni, Zn-Co alloy etc. which provides excellent corrosion resistance when used as coating material on mild steel. Further improvements on the corrosion resistance of mild steel are still being sought, since mild steel is one of the world's most useful materials. A promising solution to this is the development of Zn–Al alloy composite on mild steel. Research works in this area are however

very scarce. [11] codeposited $Al_2O_3$ in the Zn–Ni matrix and reported that the incorporation of $Al_2O_3$ increased the Ni content in the Zn–Ni matrix which resulted in a higher anticorrosion behaviour, good surface morphology than when pure zinc was used. The marine industry has shown increasing interest in Zn–Al electrodeposition as a substitute for toxic and expensive cadmium or nickel coatings [9-12]. The amount of aluminum generated from 10% by weight of $Al_2Cl$, will give corrosion protection five times superior to that obtained with pure zinc deposit even with other codeposition metals [8–15]. Although aluminum is a light in weight than zinc, the codeposition of Zn–Al is strongly anomalous in nature. However, the nucleation growth, mechanical and adhesion mechanism have not been studied in details, most especially in chloride and hydroxide environments [16-19]. In this work, an effort has been made to develop a bright and adherent zinc–aluminum alloy deposition on mild steel using powder particles of these metals. The morphological features, mechanical, corrosion, and adhesion properties of the developed coatings will be investigated.

## 2. EXPERIMENTAL METHOD

The electroplating of Zn-Al was achieved in an electroplating cell consisting of three electrodes. Locally sought mild steel of (40 mm x 20 mm x 1 mm) sheet was used as substrate and zinc sheets (30 mm x 20 mm x 1 mm) were used as anodes. The chemicals used were of analar grade and easily soluble in water. Distilled water was used for the preparation of solutions. The bath contain 50 g each of 98.5 % pure aluminum and 98.8 % zinc powder which were put into a 250 ml bottom flask and dissolve in 50 ml of NaOH, 50 ml of 5 % nitric acid. Thereafter, the surface preparation was carried out. The samples were polished with different grades of emery paper in order of 60 μm, 120 μm, 360 μm, 400 μm and 1600 μm then cleaned with $Na_2CO_3$ solution. Acid pickling operation in 20% 0.5 M HCl was used for descaling and finally activated by dipping in 10% HCl solution at room temperature for 15 seconds followed by rinsing in distilled water. Cathode and Anodes were connected to the D.C. power supply through a rectifier at 2 A. Electrodeposition was carried out at varying applied voltage between 0.6-1.0 V for 20 minutes. More so, the immersion depth was kept constant. Finally, the samples were rinsed in water to wash the salt and oxide solution off the plated samples immediately after the electroplating process. The rinsing was done in distilled water for 5 second then later air dried. Morphological study of the Zn-Al composites coating deposited at different applied potential was investigated using Scanning electron microscope (SEM/EDS) and Atomic force microscope AFM. The corrosion resistance verification of the deposited Zn-Al coatings was investigated in 3.65% NaCl using the potentiodynamic polarization technique.

## 3. RESULTS AND DISCUSSION

Experimental results obtained for Zn-Al electro-deposition are shown in Table 2. The deposition time and voltage were varied during deposition to achieve good coating thicknesses. Table

2 displays the electro-deposition data. The type of surface texture achievable depends on the composition of electrolyte and substrate, the potential and other parameters.

Following the Zn-Al deposition, a good surface thickness was achieved from the deposition bath. This is because applied voltage is inversely proportional to the time of deposition during surface coating.

**Table 1.** Summarized data of Zn-Al plated samples for constant plating time at various voltages

| Sample No | Deposition Time (min) | Deposition Voltage (V) | Plating Effects |
|---|---|---|---|
| Zn-Al 1 | 20 | 0.6 | Diffused reflection |
| Zn-Al 2 | 20 | 0.7 | Diffused reflection |
| Zn-Al 3 | 20 | 0.8 | Diffused reflection |
| Zn-Al 4 | 20 | 0.9 | Bright reflection |
| Zn-Al 5 | 20 | 1.0 | Bright reflection |
| Zn (As-received) | 20 | - | - |

*Material Characterization*

Figure 1 show a SEM micrograph and EDS of the Al particles which were used for the bath formation and co-deposition of Zn-Al alloy. Most solutions and powders admixed during electrodeposition of metals and alloys contain one or more inorganic or organic additives that have specific functions in the deposition process. Al powder purity was determined by EDS spectrum showing high peak. This proves that the powder used was pure and free from contamination.

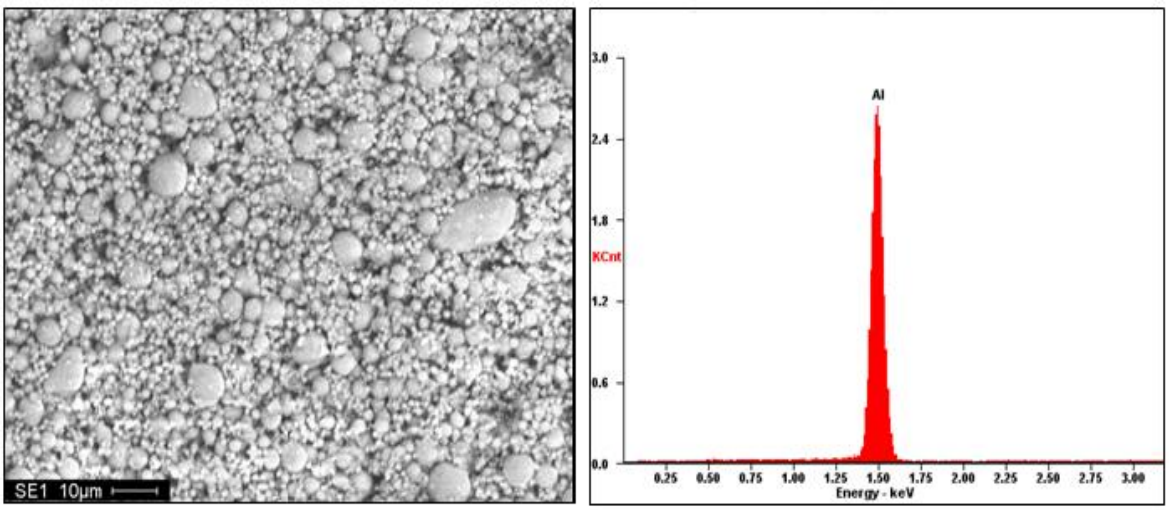


**Figure 1.** SEM/EDS spectra Al

*Atomic force microscope of Zn-Al deposition*

Atomic force microscope photomicrography was used to analyze the nature of crystal growth, adhesion properties and the surface roughness of the plated samples made at different applied voltages. AFM photomicrographs obtained from the Zn–Al coatings on mild steel are shown in Figure 2 - 4.

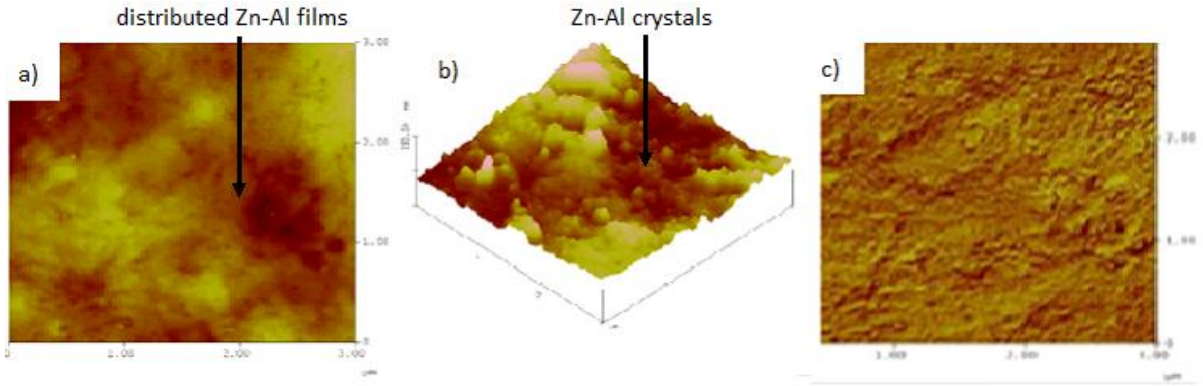


**Figure 2.** AFM images of the Zn-Al film obtained for sample 1; (a) 2-D image, (b) 3-D relief image and (c) roughness analysis**.**

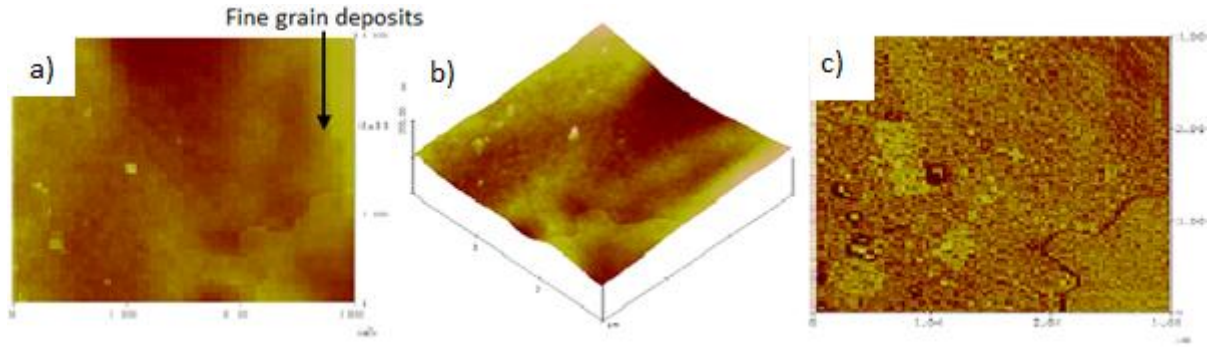


**Figure 3.** AFM images of the Zn-Al film obtained for sample 3; (a) 2-D image, (b) 3-D relief image and (c) roughness analysis

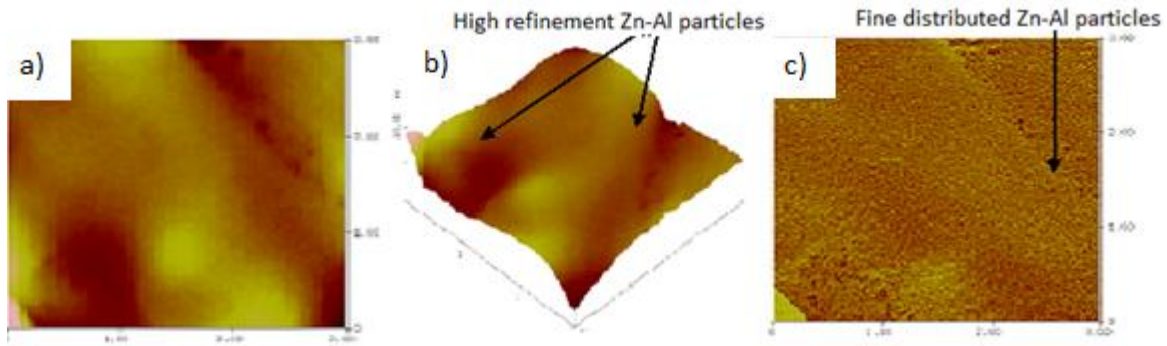


**Figure 4.** AFM images of the Zn-Al film obtained for sample 5; (a) 2-D image, (b) 3-D relief image and (c) roughness analysis

Comparing these micrographs, it was observed that the sample 1 (Figure 1) shows a distribution of Zn-Al intermetallic particles with coarse–grain formation having non uniform crystal size. According to [12] the surface roughness increases significantly with the film thickness. This study shows that it is not in all cases. However, one can say that the surface roughness and adhesion increases as a result of applied voltage on the deposited metal because film thicknesses are influenced by particle size distribution, distance between anode and cathode, depth of immersion etc., as stated by [1, 2 and 10]; which is in conformity with the principles of deposition. In Figure 2, fine grain size and uniform crystal growth was achieved. This observation implied that the more cathodic the deposition potential, the smoother the Zn–Al film, since refining of the crystallites took place. According to [20], deposition films obtained within 1-1.4 V mostly covered the substrate and exhibited coalesced crystallites. However, high refinement of crystal growth and uniform arrangement of the distributed crystals was achieved more in Figure 4 which is in line with the [18-20] opinion on binary alloy. It is also noteworthy to say that the porous-free nature of the coating and the change in morphology of Zn-Al 5 (Figure 4) can be linked to a strong penetrating effect of Al migration from the bath which causes an increased surface nuclei topography arrangement, strong surface adhesion hence promoting the formation of smooth and shiny intermetallic coatings.

*Solid XRD analysis of Zn-Al deposited mild steel*

Figures 5, 6 and 7 show the solid XRD spectra for Zn-Al deposited samples. Phase composition of the surface layers of the Zn-Al coatings was compared and all the samples showed exactly the same or similar phases as seen in the spectra. From the profiles, phases shown are: $Al_4Zn$; $Al_3ZnO_2$; *Al-Zn* and *Al*. However, some of the phases have high peaks of $Al_3ZnO_2$. The reaction between aluminium and zinc inside the admixed bath during deposition on mild steel resulted in zinc-aluminide intermetallic precipitates thereby producing fine grain microstructures. The XRD patterns of the deposited substrates showed some similarities; for Figure 6 and Figure 7.

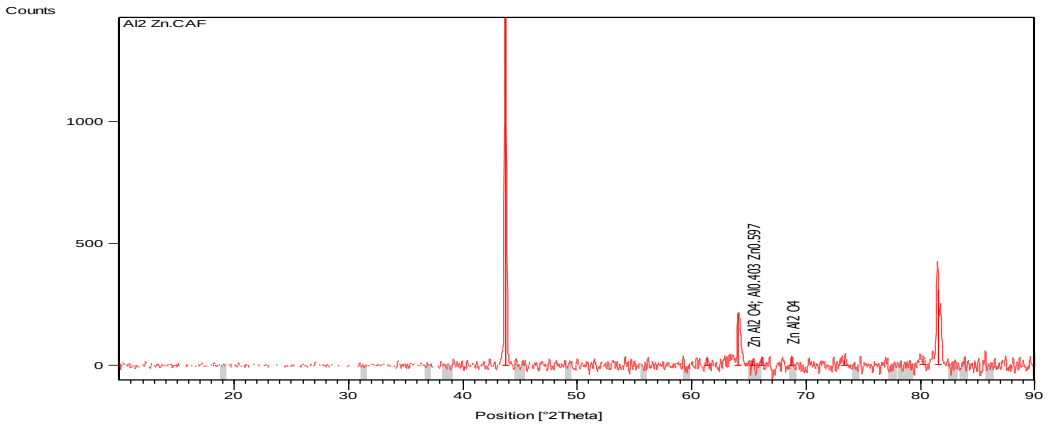


**Figure 5.** Solid X-ray diffraction profile for Zn-Al 1

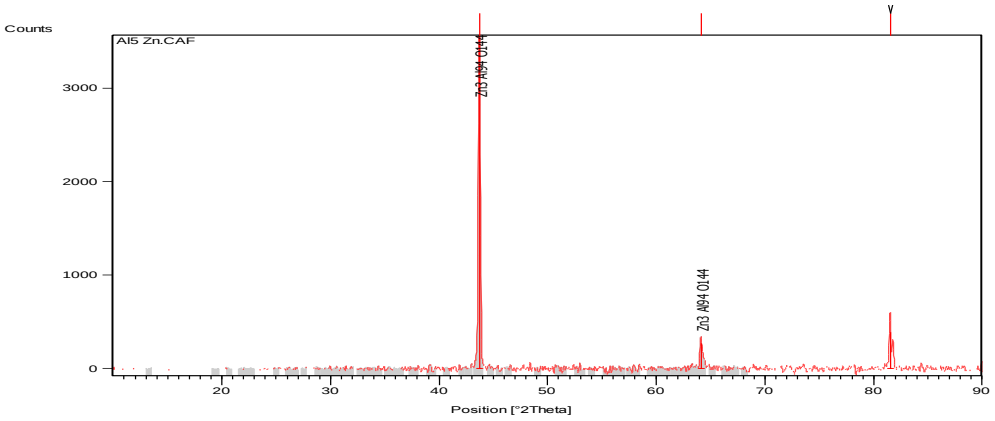


**Figure 6.** Solid X-ray diffraction profile for Zn-Al 3

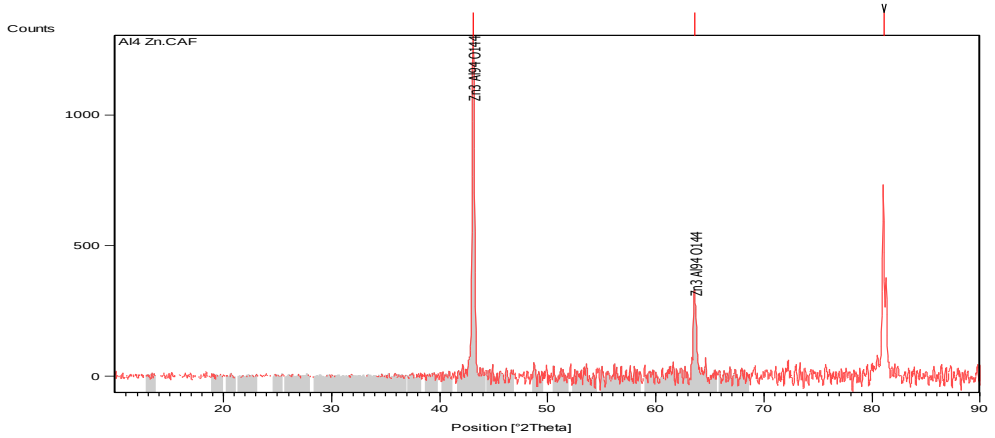


**Figure 7.** Solid X-ray diffraction profile for Zn-Al 5

However, significant differences in their peak levels affirm the bonding effect. The similarities in their patterns confirmed the presence of Al particle deposit while the differences in their peaks could be as a result of the variation in the rate of deposition.

*SEM/EDS analysis of Zn-Al deposited mild steel*

Surface morphology of the Zn-Al coatings developed at different applied voltages was investigated using Focus ion beam scanning electron microscope (FIB-SEM). The morphology of deposited Zn-Al coatings in terms of its uniformity, presence of porosity, grain size and stress developed were examined in Figures 8-10.

The SEM images of the coatings deposited from Zn-Al 1 (Figure 8) plated at low applied voltage (0.6 V) shows a large, dull and scattered crystal grains within the surface of the deposited samples. Reason being that, at the beginning of the electrodeposition, the rate of deposition is slow at low applied potential; alloy deposited have a large number of tiny particles on the cathode's surface which produced the cluster shown.

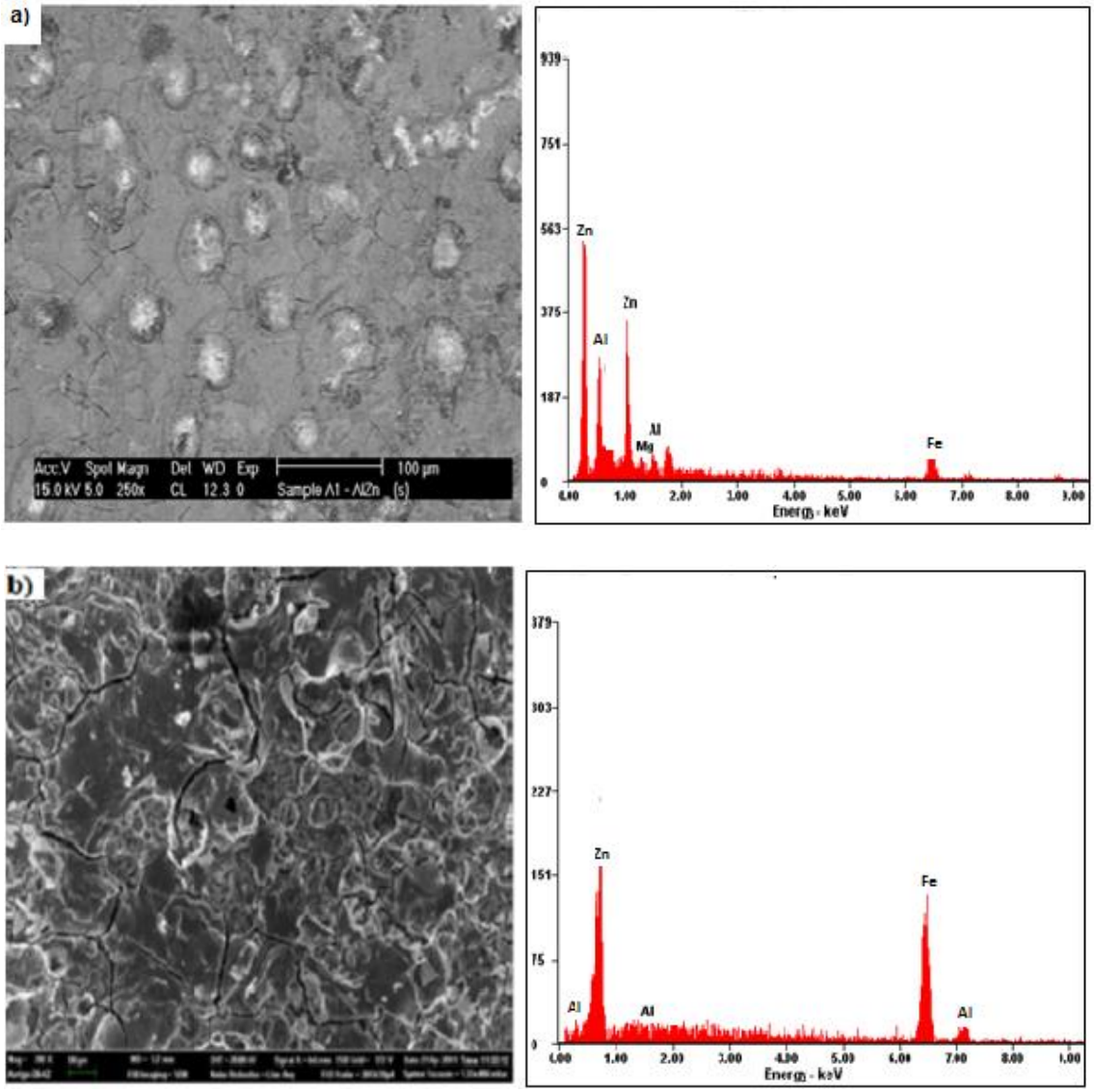


**Figure 8.** SEM/EDS of Zn-Al 1 showing (a) the surface morphology and (b) cross section of the deposited sample.

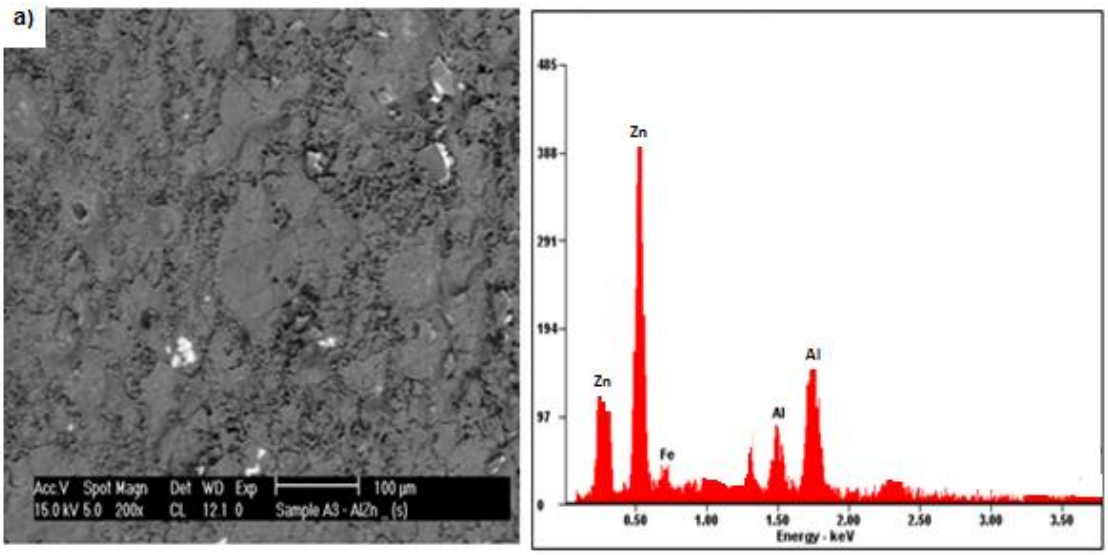

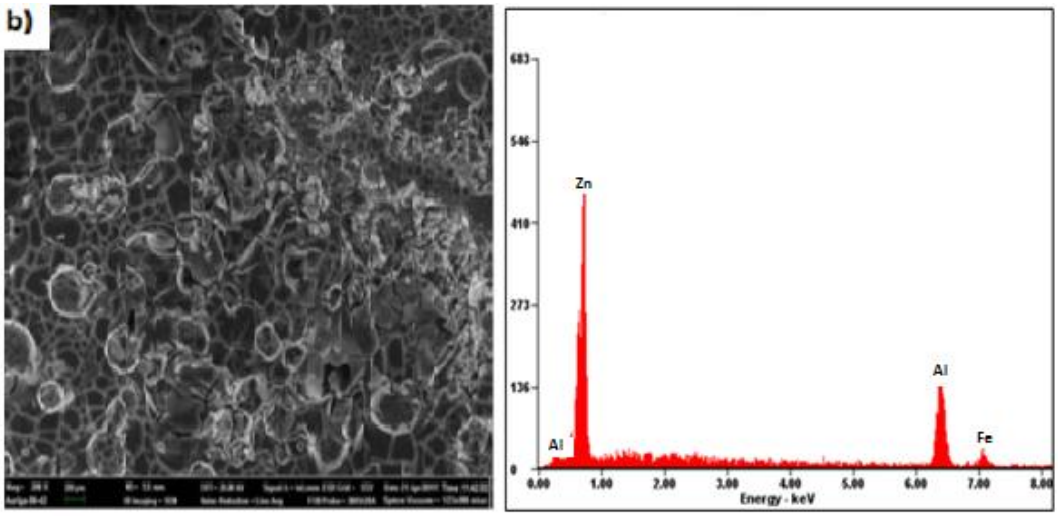


**Figure 9.** SEM/EDS of Zn-Al 3 showing (a) the surface morphology and (b) cross section of the deposited sample.

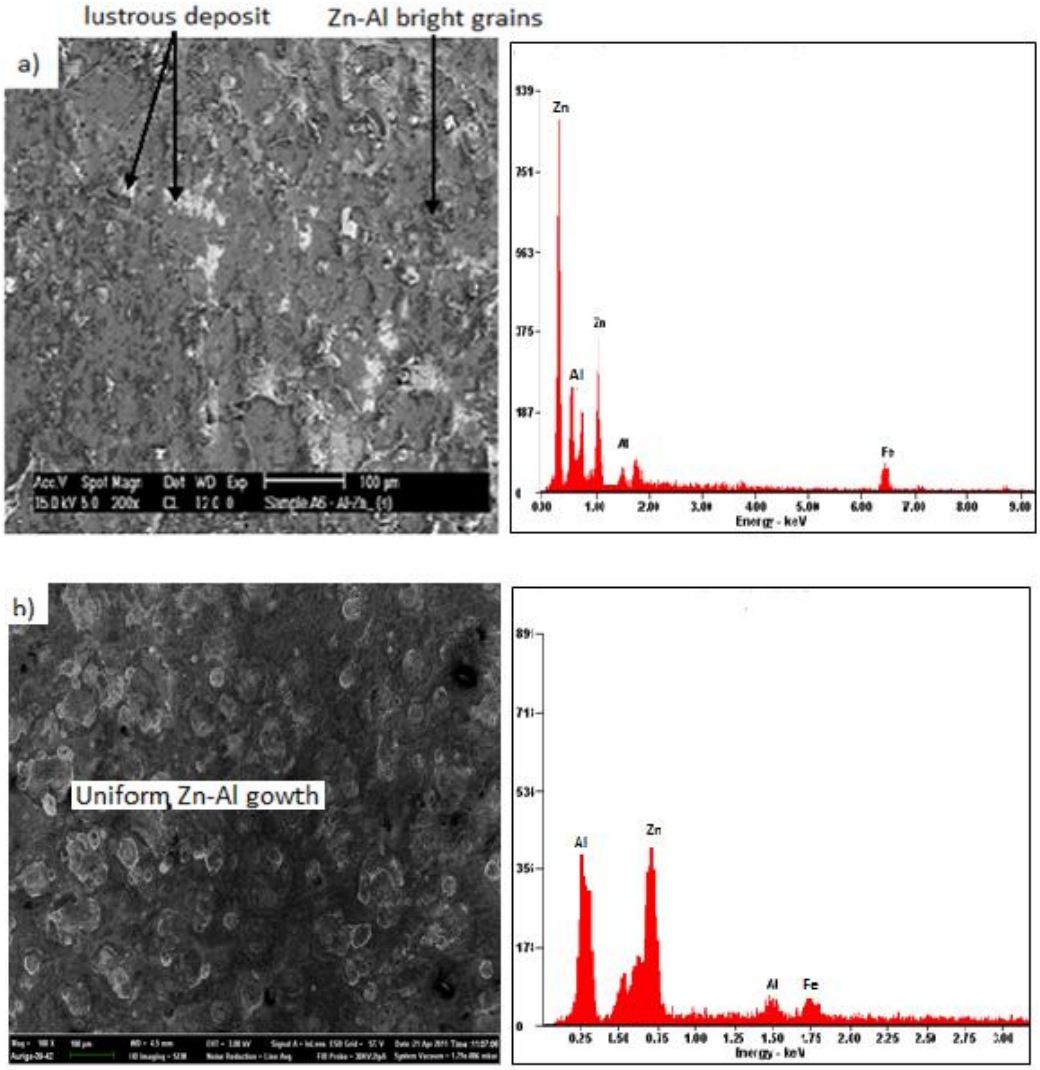


**Figure 10.** SEM/EDS of Zn-Al 5 showing (a) the surface morphology and (b) cross section of the deposited sample.

The morphological growth and surface finish of sample 3 in Figure 9 had the formation of a more densely packed corrosion product layer on coating surface, which enhanced the corrosion resistance. Thus the nature of the deposit is found to be uniform and adherent. Increasing the applied potential to 1.0 V, Zn-Al 5 was also observed to possess regular crystal size with lustrous deposit and bright grains.

No porosities was visible in the coating as seen from Figure 10, which is attributed to the effect of the applied voltage on coating structure that tends to influence the perfect grain size and porosity free deposit obtained.

Figures 11 - 13 shows the optical micrographs of the Zn-Al electrodeposited samples. The distribution of the particles in the steel can be seen in the micrographs indicating homogeneous deposition of particles was achieved.

*Fourier transforms infrared (FTIR) analysis for Zn-Al*

Figures 14, 15 and 16 show the FTIR spectra of deposited samples. The test was carried out to obtain information about the stability of the surface films. FTIR spectra of Zn-Al deposition shows an absorption peak within 1500 -1800 $cm^{-1}$ for Zn-Al 5 (see Figure 16) at 20% range of transmittance. From all indications, Al film covered the steel surface and according to [1] these films are preferentially adsorbed on the peak of the dendritic growth sites, preventing further growth of their peaks, leading to a smoother surface.

An absorption band revealing the slight vibrational properties of Zn ion and $Al(OH^-)_4$ is observed for each Zn-Al samples (see Figures 14, 15 and 16) in the range 400–4000 $cm^{-1}$. More so, common bands exist in all cases, such as the OH band which centered on 1000 $cm^{-1}$ – 1500 $cm^{-1}$ at 80% for sample 5 (Figure 16), 1400 $cm^{-1}$ – 1600 $cm^{-1}$ at 60% for sample 3 (Figure 15) and 1500 $cm^{-1}$ – 1800 $cm^{-1}$ at 20% for sample 1 (Figure 14).

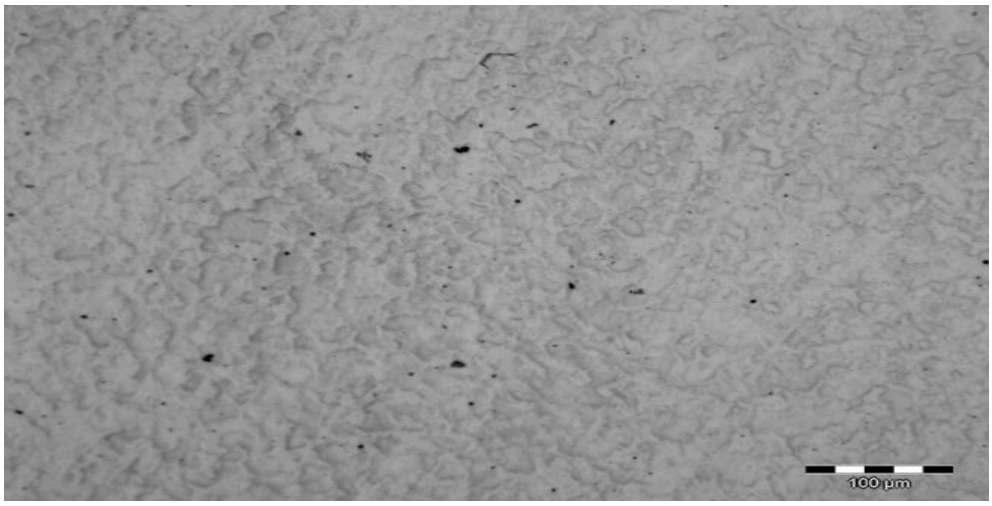


**Figure 11.** Optical micrograph of the cross section of Zn-Al deposited mild steel at 0.6 V, 20 min.

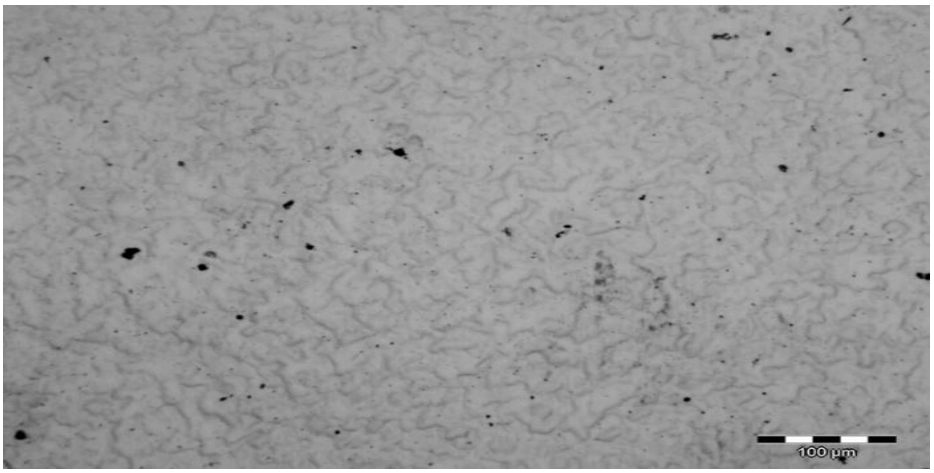


**Figure 12.** Optical micrograph of the cross section of Zn-Al deposited mild steel at 0.8 V, 20 min.

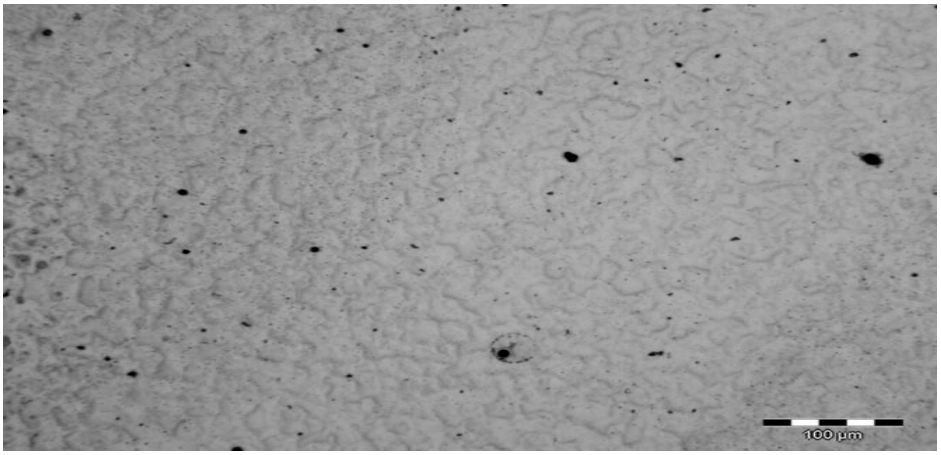


**Figure 13.** Optical micrograph of the cross section of Zn-Al deposited mild steel at 1.0 V, 20 min.

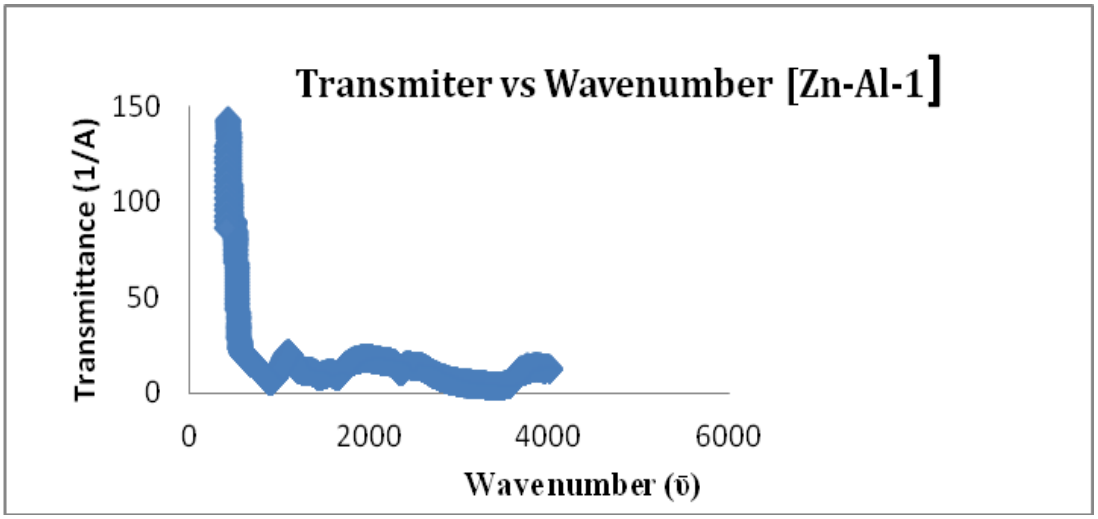


**Figure 14.** Fourier transform infrared spectroscopy of Zn-Al deposited mild steel at 0.6 V, 20 min.

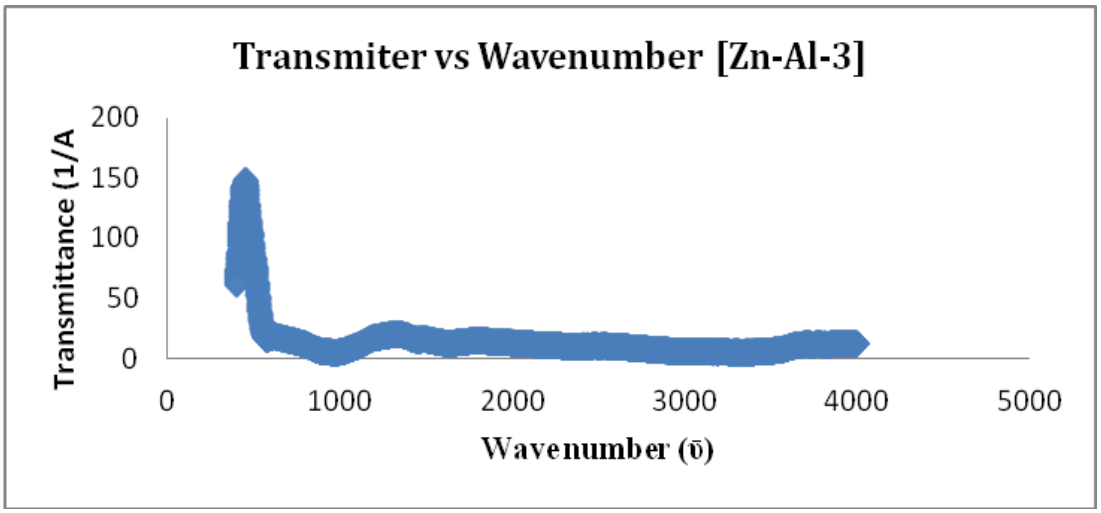


**Figure 15.** Fourier transform infrared spectroscopy of Zn-Al deposited mild steel at 0.8 V, 20 min.

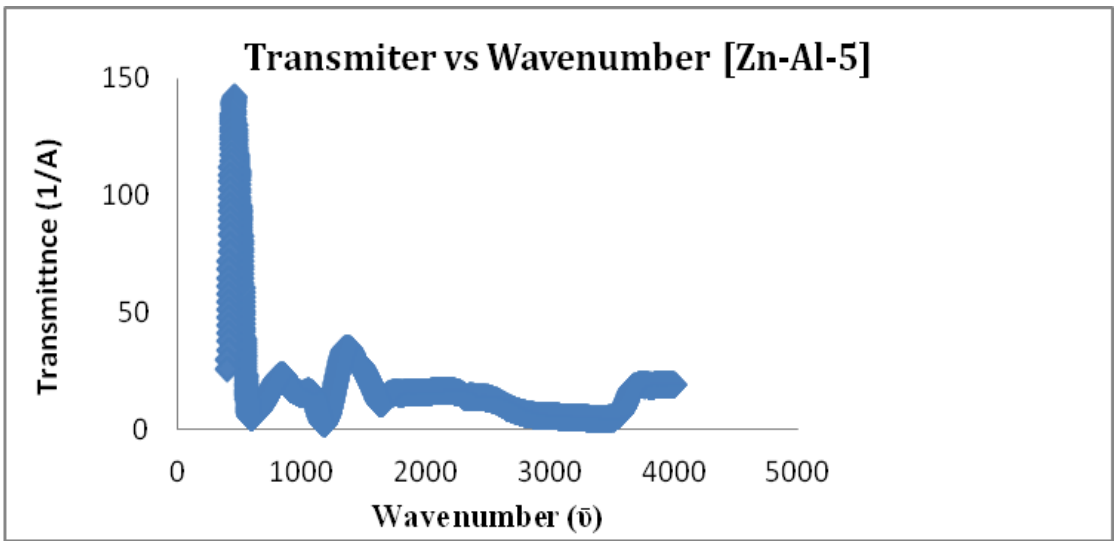


**Figure 16.** Fourier transform infrared spectroscopy of Zn-Al deposited mild steel at 1.0 V, 20 min.

To validate the qualities of electrodeposition obtained, the difference in brightness from Figure 15 and 16 is a function of relative flatness of the surface and the applied potential value with regard to the wave number. Experimental result clearly shows that the grains making up the surface are much smaller, making the surface macroscopically flatter and more homogeneous as seen in Figure 16.

*Microhardness Analysis*

The microhardness (HVN) value of the deposited coatings for each sample at different applied potential was measured. From all indications, hardness increased from 55 HVN for base mild steel to approximately 130 HVN (cross-section) for the deposited Zn-Al 1 (see Figure 17).

The variation of microhardness as a function of distance from the substrate–coating interface was examined and the average microhardness values for all the samples were calculated. Zn-Al 5 has the highest value of hardness (see Figure 17). This was due to the influence of plating voltage that was applied during deposition in the bath. This improvement in hardness of deposited Zn-Al samples (over double the microhardness of substrate) especially with Zn-Al 3 and Zn-Al 5 was attributed to the formation of adhesive properties from solid solution of Zn and Al after coating. This is in line with the study carried out by [11, 12] and [18] that higher hardness of the coating developed can be attributed to the fine-grained structure of the deposit or alloys and the dispersed particles in the fine-grained matrix which may obstruct the easy movement of dislocations. More so, three regions are distinguishable on the curve: a region of initial deposit, a middle region and a region of final output deposit. The improved microhardness values were due to the presence of Al in the electrodeposition bath.

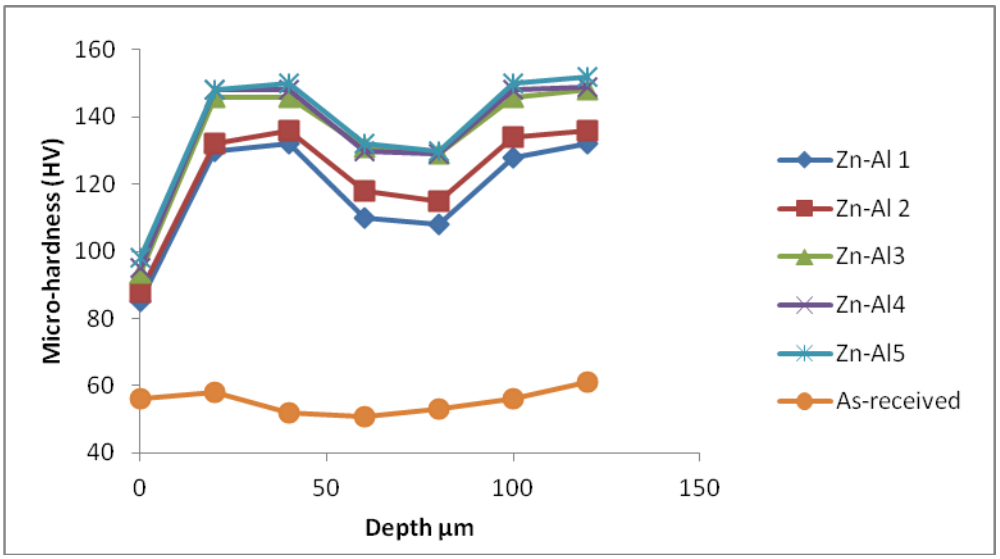


**Figure 17.** The microhardness/depth profile for Zn-Al deposited sample

*Wear Rate Evaluation of Zn-Al Deposited Mild Steel*

The wear study of Zn-Al deposited samples was carried out. Figures 18 and 19 shows the graphs of the variation of the wear mass loss and wear rate as a function of time for all the samples (as-received and Zn-Al depositions) respectively. The rate of wear is very high for the as-received sample; whereas, the rate of wear is very low for the Zn-Al samples especially with Zn-Al 5 (see Figure 19). This may be attributed to the high degree of particles migrated from the bath due to the influence of applied voltage. Best wear resistance was displayed by Zn-Al 5. More so, it can also be said that the presence of aluminum enhanced the wear resistance and reduced wear mass loss as observed in Figure 19. Furthermore, wear was evaluated by analyzing the wear morphology on the surfaces of the deposited Zn-Al samples and the substrate.

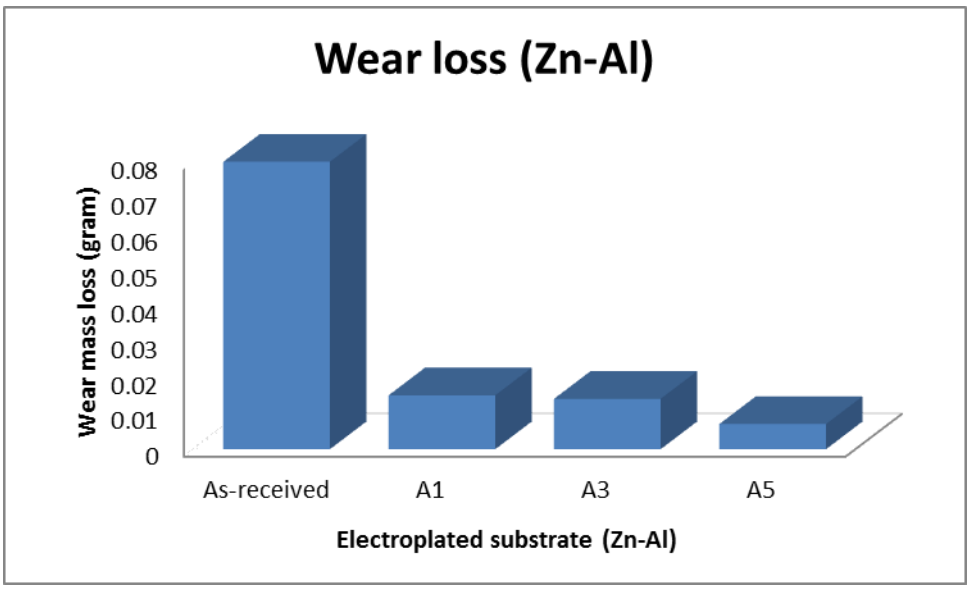


**Figure 18.** Variation of the wear mass loss with time

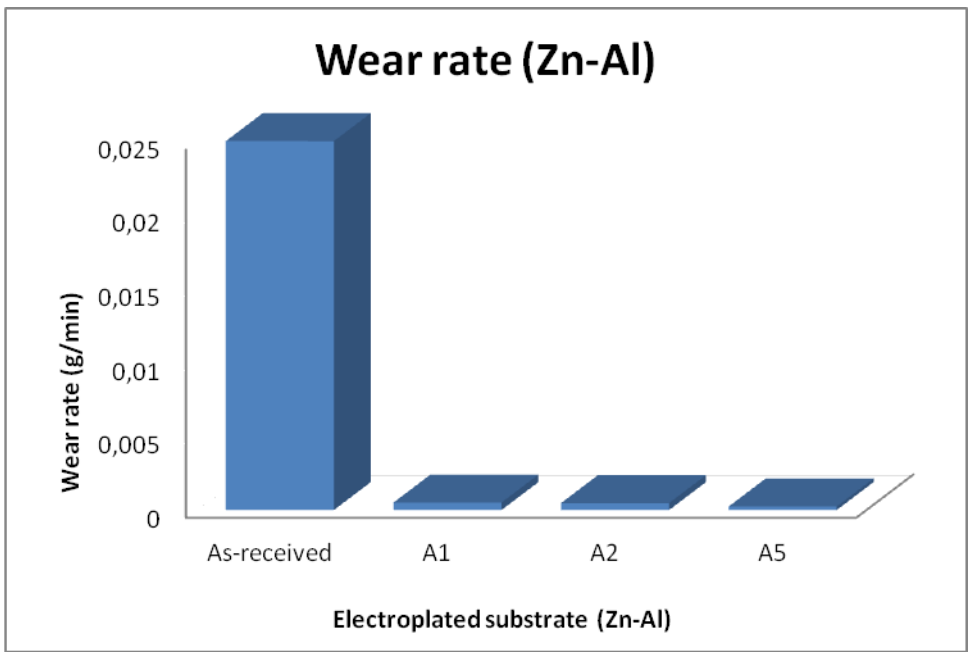


**Figure 19.** Variation of the wear rate with time

The wear scar morphology of the Zn-Al depositions was used to establish the stability of coatings on the substrate. Figures 21, 22 and 23 shows the worn surfaces of the samples. From the SEM images, little degree of plastic deformation, massive grooves, pits and fracture can be seen on the surface of the as received sample as shown in Figure 20.

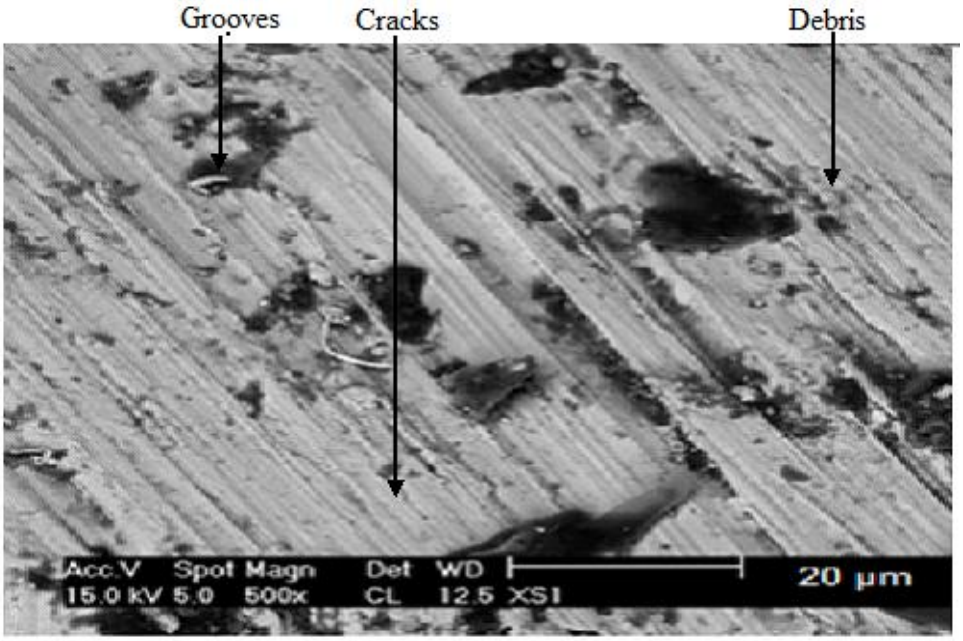


**Figure 20.** SEM images of the wear scar of mild steel

Zn-Al 1 was observed to have a better appearance (Figure 21), compared with the mild steel indicating slightly weak adhesion between the Zn-Al deposit and the steel. However, lesser degree of plastic deformation, grooves and little pull-out can be seen on the Zn-Al deposited samples 3 and 5 (Figure 22 and 23). The zinc–aluminium alloys have a multiphase structure consisting of mainly aluminium-rich and zinc-rich phases. In addition, oxide films are formed on the surface of zinc–aluminium alloys during dry sliding which contribute to their excellent wear resistance. According to [19] the formation of oxide films on the wear surfaces of these alloys provide a higher wear resistance.

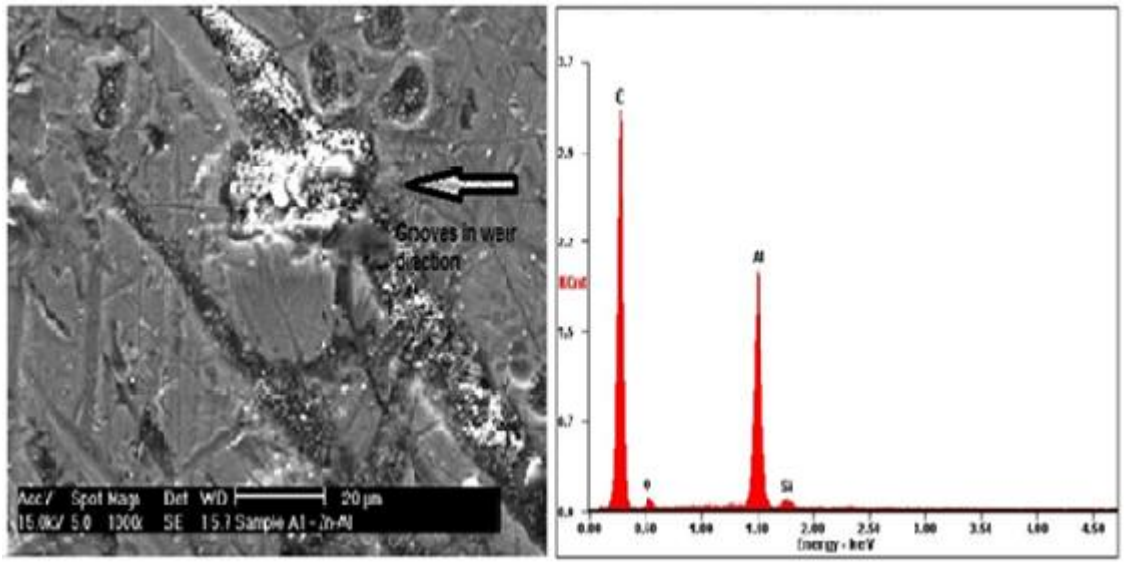


**Figure 21.** SEM/EDS images of the wear scar of Zn-Al 1

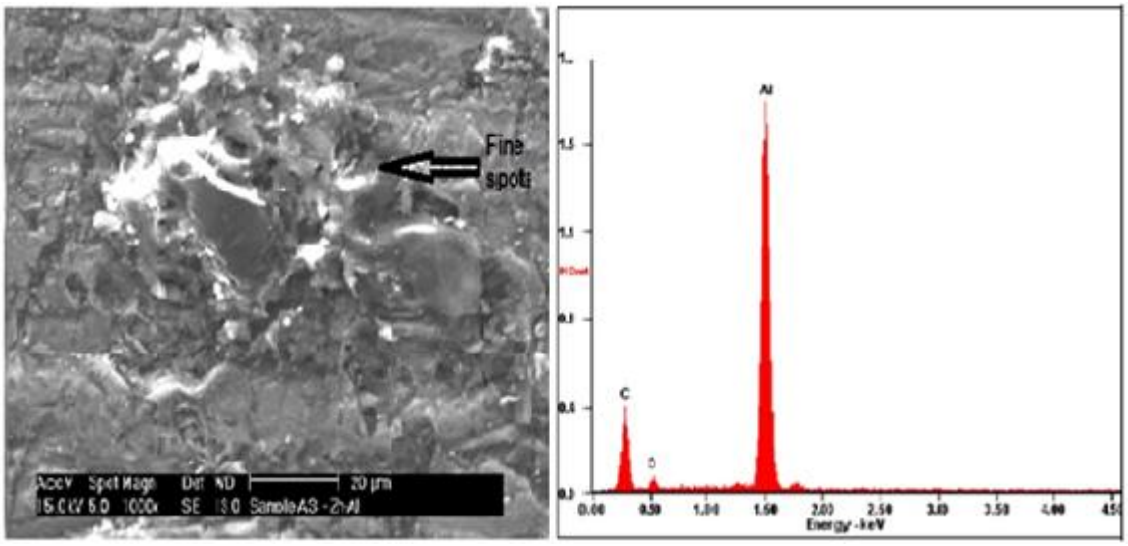


**Figure 22.** SEM/EDS images of the wear scar of Zn-Al 3

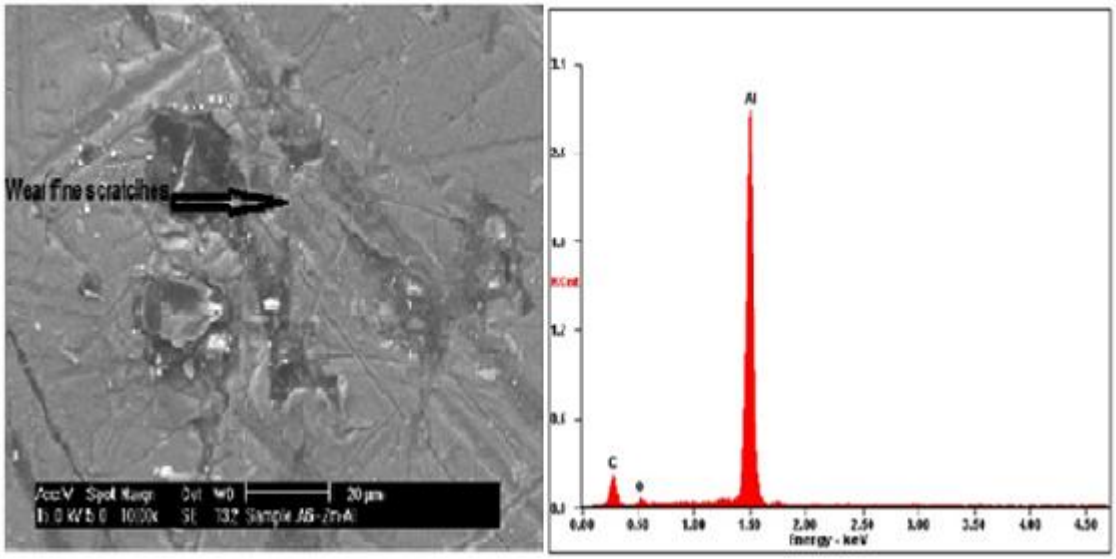


**Figure 23.** SEM/EDS images of the wear scar of Zn-Al 5

Aluminium oxide is a hard ionic compound and therefore acts as a load-bearing phase. In addition, it was seen that the width and depth of the wear scars on the Zn-Al 3 and 5 samples are much smaller than that of the Zn-Al 1 and the as-received samples under the same wear conditions. It should be noted that the stable cohesion of the former has a better flow than the visible irregular degradation of the later.

*Electrochemical Test Result*

The electrochemical properties of the Zn-Al coatings were examined. The corrosion behaviour of the Zn-Al samples was measured using a linear potentiodynamic scan and open circuit corrosion

potential measurements technique in 3.65% NaCl. The variations in the OCP values of the samples were studied at zero applied current immediately after the immersion of the coated samples in the different media for one hour. The variation in open-circuit potential as a function of time for Zn-Al 1, 2, 3, 4 & 5 and mild steel tested in 3.65% NaCl are presented in Figure 24. The potential was observed to shift towards positive values for all the samples except for the substrate that moves drastically toward more negative region. The negative shift of the potential indicated the strong dissolution of the mild steel due to the absence of passivation. It is significant to mention that the positive shift of the potential indicates the formation of protective films and an increase in the passive film thicknesses.

From all signs, Zn-Al 5 as seen in Figure 24 tends to form more stable passivity than the other coatings due to the large number of tiny particles deposited on the cathode at higher applied voltage.

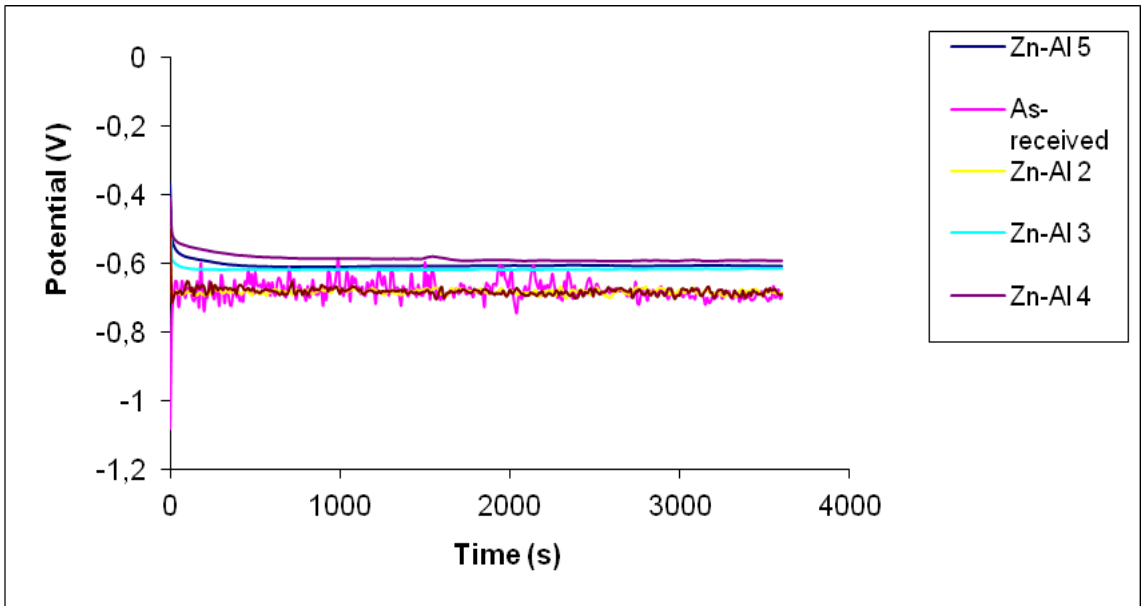


**Figure 24.** Open circuit potential curves of Zn-Al deposited mild steel

The results of polarization measurements for the specimens investigated are summarized in Table 3.

**Table 3.** Summary of the potentiodynamic polarization results

| Sample | $i_{corr}$ (A) | $I_{corr}$ (A/cm$^2$) | $R_P$(Ω) | $E_{corr}$ (V) | Corrosion rate (mm/yr) |
|---|---|---|---|---|---|
| As-received | $2.04x10^{-3}$ | $7.04x10^{-2}$ | $2.76x10^{2}$ | -1.536 | 41 |
| Zn-Al 1 | $2.64x10^{-5}$ | $1.5x10^{-4}$ | $2.89x10^{3}$ | -0.563 | $8.3x10^{-2}$ |
| Zn-Al 2 | $2.30x10^{-5}$ | $1.4x10^{-4}$ | $2.97x10^{3}$ | -0.567 | $8.5x10^{-3}$ |
| Zn-Al 3 | $5.42x10^{-6}$ | $3.3x10^{-5}$ | $2.04x10^{4}$ | -0.701 | $1.9x10^{-5}$ |
| Zn-Al 4 | $4.43x10^{-7}$ | $2.7x10^{-6}$ | $1.37x10^{5}$ | -0.731 | $1.6x10^{-5}$ |
| Zn-Al 5 | $5.74x10^{-8}$ | $3.5x10^{-7}$ | $1.38x10^{5}$ | -0.768 | $2.0x10^{-7}$ |

It was also observed from the polarization curves that the corrosion resistance of Zn-Al alloy coating increases with increase in applied voltage and obviously this might be as a result of the proportion of weight/thickness attained for all samples during deposition. In case of Zn-Al 1 the corrosion rate decreases greatly with presence of the Zn-Al in a steel matrix for Zn-Al 3 and Zn-Al 5 the corrosion rate decreases more than Zn-Al 1 due to the buildup of strong adhesive films. Hence, these phenomena show that the Zn-Al content in the deposited alloy strongly increases the corrosion resistance of the coatings. The corrosion potential of deposited samples for Zn-Al 5 is -0.768 V while that of mild steel is -1.536 V. This implies that corrosion potential increased with 0.768 V and this increase may be traced to the presence of the deposited particles. Additionally, deposited samples displayed greatly reduced corrosion current in all instances as compared to the mild steel. From the polarization results, mild steel had a corrosion current of $2.04x10^{-3}$ A and Zn-Al 5 displayed $i_{corr}$ of $5.74x10^{-8}$ A, this means a five orders of magnitude decrease in corrosion current was achieved. Also, mild steel exhibited highest corrosion current density ($7.04x10^{-2}$ A/cm$^2$) than all deposited samples, while Zn-Al 5 has $I_{corr}$ of $3.5x10^{-7}$ A cm$^{-2}$, a five order magnitude decrease in corrosion current density was attained due to the effects of electrodeposition on mild steel. Polarization resistance ($R_p$) for Zn-Al 5 is $1.38x10^5$ Ω which was the highest attained for all coated samples. Three orders increase in magnitude was attained when compared with $2.76x10^2$ Ω for as received sample.

From the polarization behaviour in Figure 25, it can be stated that corrosion resistance of the mild steel is enhanced drastically with the addition of aluminum rather Zn alone as electrodeposition material due to the formation of passive film containing $Al^{3+}$ *and* $Zn^{2+}$ which are active barriers against surface degradation.

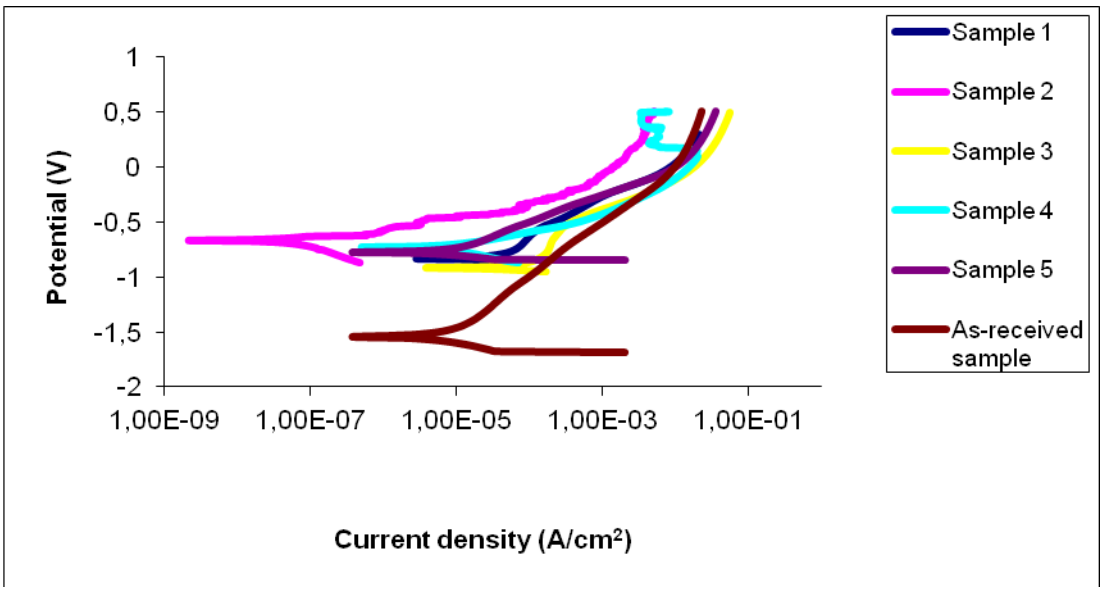


**Figure 25.** Potentiodynamic polarization curves for Zn-Al deposited mils steel

Detailed inspection of coated surface of Zn-Al samples using AFM after corrosion test also revealed the existence of irregularities and surface imperfection that exist. Figure 26 indicates that Zn-

Al 1 has few pits formed on the surface compared to the rest of the samples. [5] Categorically put that the morphological characteristics of deposited coating depend on the applied voltage, bath composition and the additives.

According to [21], since the deposition rate is slow at low applied voltage, at the beginning of the electrolysis, alloy deposits has a large number of tiny particles on almost all over the cathode surface which acts as nucleation for further deposition at the preferential sites.

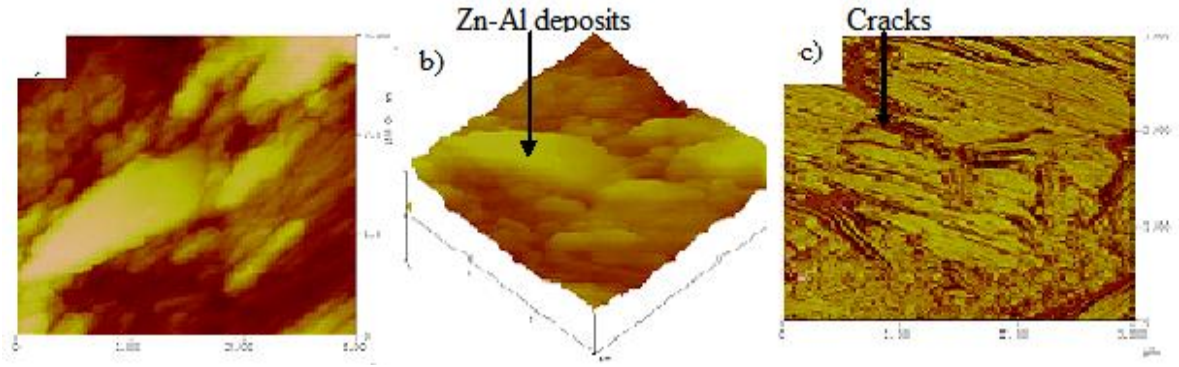


**Figure 26.** AFM images of the Zn-Al 1 after corrosion.

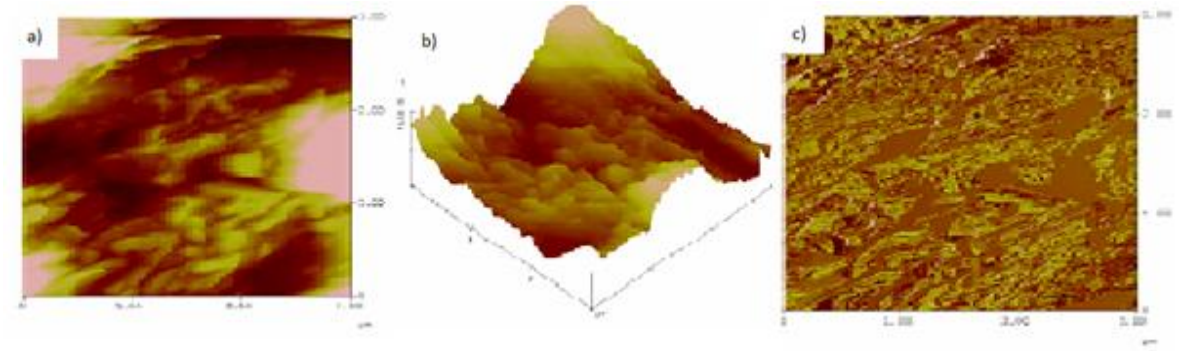


**Figure 27.** AFM images of the Zn-Al 3 after corrosion.

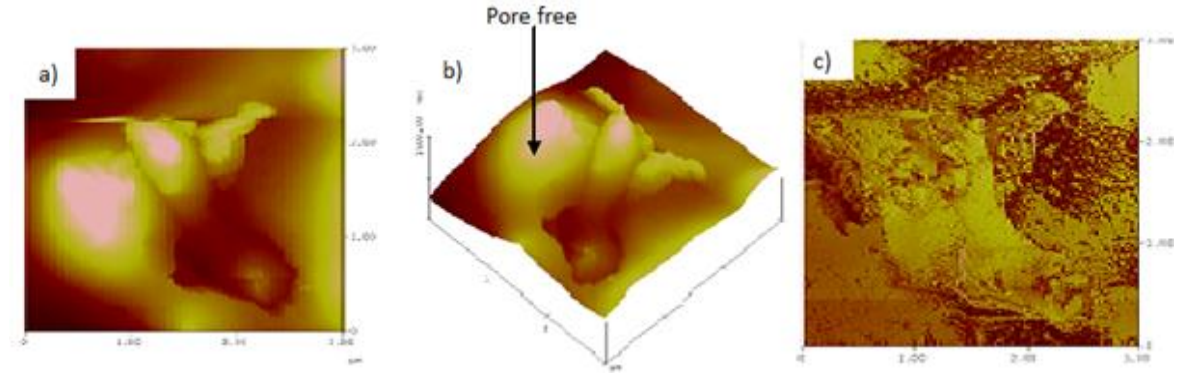


**Figure 28.** AFM images of the Zn-Al 5 after corrosion.

## 4. CONCLUSION

Co-deposition of Zn-Al was successfully carried out on mild steel surface by electroplating method. Surface morphology, microhardness and corrosion resistance of the coated samples were investigated with the following deductions:

- The microhardness value of the mild steel increased greatly due to the presence of Zn-Al particles: from 55 HVN for the substrate to 137 HVN for Zn-Al 5. The microhardness of the coated sample clearly increased over two times as much as the base material.
- The wear resistance of the coated samples also increased significantly.
- The electrochemical study revealed that corrosion resistance of mild steel was improved after zinc-aluminium deposition. The sample produced with the highest applied potential had the highest Zn-Al particles deposited and well dispersed on its surface. This sample also displayed the highest microhardness value as well as corrosion resistance.

ACKNOWLEDGEMENT
The author acknowledges the financial support of Tshwane University of Technology, provision of electroplating equipment by TIA (Technological Station in Chemical, Garankuwa) and the contribution of Mr. Abel Chuma and Miss Mapule (Queen).

## References

1. S. Shivakumara, U. Manohar, Y. Arthoba Naik, & T. U. Venkatesha,. *Bull. Mat. Sci*. 30 (2007) 455
2. M.O.H. Amuda, W. Subair, and O.W. Obitayo. *Int. J. of Eng. Research in Africa*, 2(2009)31
3. N. Pedro De Lima, N. Adriana, P. Correia, and S. A. Walney, *J. Brazil Chem. Soc*. 18, (2007)1164
4. A.P.I Popoola and O.S. Fayomi *Int. J. of Electrochem. Sci*., 6, (2011)3254
5. M.J. Rahman, S.R. Sen, M. Moniruzzaman, and K.M. Shorowordi, *J. of Mech. Eng, Tran*., 40, (2009) 9.
6. A.A. Volinsky, J. Vella, I.S. Adhihetty, V.L. Sarihan, L. Mercado, B.H. Yeung, and W.W. Gerberich, 2001. *Mat. Res. Soc*., 649, 1-6
7. A.P.I Popoola and O.S. Fayomi, *Sci Res. and Ess*., 6, (2011) 4264-4272.
8. I.U. Hague, N. Ahmad, and A. Akhan, *J. of Che. Soc. Pakistani*, 27, (2005) 337.
9. Z. Huan-Yu, A. Mao-Zhong, L. Jun-feng. *Appl. Surf. Sci*., 254 (6) (2008) 1644.
10. O.S. Fayomi, V.R. Tau, A.P.I. Popoola, B.M. Durodola, O.O. Ajayi, C.A. Loto, and O.A. Inegbenebor,. *J. of Mat. and Env. Sci*., 3, (2011) 271
11. A.P.I. Popoola, S.L. Pityana, and O.M. Popoola, *J. of the South Afri. Inst. of Min and M*et., 111, (2011) 335.
12. A.P.I. Popoola, S.L. Pityana, and O.M. Popoola. *J. of the South Afri. Inst. of Min and Met*., 111 (2011) 345.
13. Princeton Applied Research. Electrochemical Division, 1-8`
14. A.P.I. Popoola, O.S. Fayomi and O.M. Popoola., O.M. 2011. *Proc. of Mat. Sci. & Tech. Conf*., Ohio: Usa. (2011) 393-400.
15. S. Basavanna, and Y. Arthoba Naik, *J. of Appl. Electrochem*., 39 (2009) 1975
16. G. Sundararajan, and L. Rama Krishna. *Surf. and Coat. Tech*, 167, (2003) 269.
17. B. Bobić, S. Mitrović, M. Babić, and I. Bobić, *Tribology In Industry*, 32(1) (2010) 3
18. B.K. Prasad, and O.P. Modi, *Trans. of Nonfer. Mat. Sci. China*, 19: (2008) 277.
19. P. Gença˘ga, S. S. Temel, K. Tevfik, & M. Samuel, 2002. *Els. Sci Wear*, 894:901.

20. G.A. Finazzi, E.M. Oliveira, and I.A. Carlos, *Surf. Coat. Tech*. 187, 2004.377
21. B.M Praveen, and T.V. Venkatesha, *Int J. of Electrochem*, 261, (2011) 407